

This document was prepared in conjunction with work accomplished under Contract No. AT(07-2)-1 with the U.S. Department of Energy.

DISCLAIMER

This report was prepared as an account of work sponsored by an agency of the United States Government. Neither the United States Government nor any agency thereof, nor any of their employees, makes any warranty, express or implied, or assumes any legal liability or responsibility for the accuracy, completeness, or usefulness of any information, apparatus, product or process disclosed, or represents that its use would not infringe privately owned rights. Reference herein to any specific commercial product, process or service by trade name, trademark, manufacturer, or otherwise does not necessarily constitute or imply its endorsement, recommendation, or favoring by the United States Government or any agency thereof. The views and opinions of authors expressed herein do not necessarily state or reflect those of the United States Government or any agency thereof.

This report has been reproduced directly from the best available copy.

Available for sale to the public, in paper, from: U.S. Department of Commerce, National Technical Information Service, 5285 Port Royal Road, Springfield, VA 22161

phone: (800) 553-6847

fax: (703) 605-6900

email: orders@ntis.fedworld.gov

online ordering: <http://www.ntis.gov/help/index.asp>

Available electronically at <http://www.osti.gov/bridge>

Available for a processing fee to U.S. Department of Energy and its contractors, in paper, from: U.S. Department of Energy, Office of Scientific and Technical Information, P.O. Box 62, Oak Ridge, TN 37831-0062

phone: (865)576-8401

fax: (865)576-5728

email: reports@adonis.osti.gov

TECHNICAL DIVISION
SAVANNAH RIVER LABORATORY

DPST-70-573

RECORDS ADMINISTRATION



AYIX

TIS FILE
RECORD COPY

DISTRIBUTION

- | | |
|--------------------------|-----------------------------------|
| 1. P. L. Roggenkamp, SRL | 10. C. H. Ice-L. H. Meyer, SRL |
| 2. F. E. Kruesi, Wilm. | 11. H. J. Groh-R. L. Folger |
| 3. J. W. Croach- | 12. S. Mirshak-J. M. Boswell |
| A. A. Johnson | 13. G. Dessauer-B. C. Rusche |
| 4. D. F. Babcock | 14. H. K. Clark-E. J. Hennelly |
| 5. L. W. Fox, SRP | 15. J. A. Smith-W. E. Graves |
| 6. O. A. Towler | 16. J. R. Hilley-R.M. Satterfield |
| 7. S. V. Topp | 17. F. D. R. King |
| 8. J. L. Crandall, AOP | 18. C. K. Paulson |
| 9. F. E. Driggers | 19. TIS File Copy |
| | 20. Vital Records Copy |

December 30, 1970

MEMORANDUM

TO: P. L. ROGGENKAMP

FROM: C. K. PAULSON *CKP*

CLASSIFICATION REVIEW FOR
DECLASSIFICATION BUT LEFT
UNCHANGED

By *(14) mjk*
Date *24/04/22*
U.S. AEC Division of Classification

ANALYSIS OF $^{236}\text{Pu}/^{238}\text{Pu}$ RATIOS IN HIGH PURITY ^{238}Pu
AND COMPARISON WITH RESULTS OF ^{237}Np IRRADIATIONS IN
THE REFLECTOR OF Cf-I

INTRODUCTION

^{236}Pu is formed in small quantities during the production of ^{238}Pu from the irradiation of ^{237}Np . ^{236}Pu is produced from ^{237}Np by two interactions:

- $^{237}\text{Np}(\gamma, n) ^{236}\text{Np} \xrightarrow[22 \text{ hr}]{\beta^-} ^{236}\text{Pu} + \text{neutrino},$
- $^{237}\text{Np}(n, 2n) ^{236}\text{Np} \xrightarrow[22 \text{ hr}]{\beta^-} ^{236}\text{Pu} + \text{neutrino}.$

Both initiating particles must have energies greater than 6.8 Mev.

Classification Cancelled

By Authority of

P. M. Merrill
Name Title Date

Although the production rate of ^{236}Pu is very small, $\sim 10^{-6}$ of the ^{238}Pu production rate, these trace amounts substantially increase the hard gamma production rate over a period of several years; therefore it is advisable that the ^{236}Pu ratio be as low as practicable. The decay chain of ^{236}Pu contains daughters which produce high energy gammas (e.g., ^{208}Tl - 2.6 Mev). For ^{238}Pu power sources to be used for body implantations a limit of 0.3 ppm is placed on the $^{236}\text{Pu}/^{238}\text{Pu}$ ratio.

This memorandum discusses an extension of the method⁽¹⁾ used to calculate the $^{236}\text{Pu}/^{238}\text{Pu}$ ratio formed in the irradiation of ^{237}Np in the Savannah River reactors. The test and production irradiations in the Cf-I charge are specifically treated although the calculational technique can be applied to any charge design.

SUMMARY

The results from the calculational procedure to determine the $^{236}\text{Pu}/^{238}\text{Pu}$ ratio can be divided into three areas; evaluation of cross sections, results of $^{236}\text{Pu}/^{238}\text{Pu}$ ratio calculations, and materials considerations in ^{237}Np target design.

Cross Sections

The (γ, n) and $(n, 2n)$ cross sections have been the primary unknowns in the calculation of $^{236}\text{Pu}/^{238}\text{Pu}$ ratios. Using the experimental values of the ratios for 6 test assemblies irradiated in the Cf-I reflector, two group (γ, n) cross sections were determined; a value of 15 mb for the energy group, 6.8 - 8.0 Mev, and 68 mb for the energy group, 8.0 - 9.5 Mev. A value of 56 mb was used for the $(n, 2n)$ cross section. The $(n, 2n)$ cross section will be determined more precisely from other irradiation experience; its value is not very significant for the reflector irradiations producing 90% ^{238}Pu .

$^{236}\text{Pu}/^{238}\text{Pu}$ Ratios

The 6 test irradiations were compared with calculations to determine the 2-group (γ, n) cross sections. The calculated and experimental $^{236}\text{Pu}/^{238}\text{Pu}$ ratios are given in Table I.

TABLE I

Calculated and Experimental $^{236}\text{Pu}/^{238}\text{Pu}$ Ratios
for 6 Test Irradiations in Cf-I

<u>Radius of Test Assembly Location, cm</u>	<u>$^{236}\text{Pu}/^{238}\text{Pu}$, ppm</u>	
	<u>Calculated</u>	<u>Experimental</u>
163	0.43	0.43
210	0.41	0.39
210	0.35	0.35
222	0.44	0.41
222	0.46	0.47
235	0.98	0.98

Agreement with experiments was forced at 2 irradiation positions; however, the resultant agreement at the 4 intermediate positions was well within experimental uncertainties. A measure of the reliability of the calculational method is the standard error of estimate, S_e^2 . The experimental and calculated values for the 6 test assemblies give $S_e^2 = 3.75$. A least squares fit to the experimental data gives $S_e^2 = 7.5$. This statistic indicates that the calculational method estimates the $^{236}\text{Pu}/^{238}\text{Pu}$ ratio in the 6 test assemblies better than a least squares approach.

By use of this method, a value of 0.30 ppm was calculated for the $^{236}\text{Pu}/^{238}\text{Pu}$ ratio in the Mark 61 irradiations, for producing 2 kg of high purity ^{238}Pu .

Materials

Reducing the $^{236}\text{Pu}/^{238}\text{Pu}$ ratio below 0.3 ppm can be attained by replacing all or part of the Al in the target by either Mg or Zr. Studies indicate that a product of 0.2 ppm could be reached. Also, 6063-Al should be used in place of 8001-Al and 1100-Al whenever possible to reduce in high energy gamma production from additives in the latter two alloys.

DISCUSSIONFormation of ^{236}Pu

The formation of ^{236}Pu can be conveniently divided into four contributions. Each of the contributions to ^{236}Pu can be calculated individually and the contributions summed to arrive at the total.

1. Internal (γ, n) Reaction

The (γ, n) reaction rate, R_1 , from γ -rays generated in the ^{237}Np assembly can be expressed as:

$$R_1 = \frac{dN_{36}^{(1)}}{dt} = \sigma_{37}^{\gamma, n} N_{37}(t) \cdot \phi_{th}(t) \cdot \phi_{\gamma}, \quad (1)$$

where: $N_{36}^{(1)}$ = atom density of ^{236}Np from internal (γ, n) reactions,

$\sigma_{37}^{\gamma, n}$ = ^{237}Np (γ, n) cross section, barns,

$N_{37}(t)$ = time dependent atom density of ^{237}Np , atoms/cm³,

ϕ_{γ} = γ flux (>6.8 Mev), from thermal neutron capture in Al of Np assembly, per unit thermal flux in Al assembly, $\gamma/(\text{cm}^2\text{-sec}-\phi_{th}(t))$,

$\phi_{th}(t)$ = time dependent thermal neutron flux in Np assembly, n/cm²-sec.

With ϕ_{γ} defined in this way, the absolute value and the time dependence of the γ -ray flux is carried by ϕ_{th} .

2. External (γ, n) Reaction

The (γ, n) reaction rate, R_2 , from γ -rays generated externally to the ^{237}Np assembly can be expressed as:

$$R_2 = \frac{dN_{36}^{(2)}}{dt} = \sigma_{37}^{\gamma, n} N_{37}(t) \phi_{\gamma}(t), \quad (2)$$

where $\phi_{\gamma}(t)$ = external γ flux (>6.8 Mev) from thermal neutron capture in core and tank wall, $\gamma/\text{cm}^2\text{-sec}$.

$N_{36}^{(2)}$ = atom density of ^{236}Np from external (γ, n) reactions.

Other quantities were defined previously:

3. Internal ($n, 2n$) Reaction

The ($n, 2n$) reaction rate, R_3 , from fast neutrons generated in fissions occurring in the ^{237}Np assembly, can be expressed as:

$$R_3 = \frac{dN_{36}^{(3)}}{dt} = (\nu_{38} N_{38}(t) \sigma_{38}^f + \nu_{49} N_{49}(t) \sigma_{49}^f) \cdot \phi_{th}(t) \cdot \phi_f \cdot N_{37}(t) \sigma_{37}^{n, 2n} \quad (3)$$

where:

ν_{38} and ν_{49} = Number of neutrons, >6.8 Mev, per fission of ^{238}Np and ^{239}Pu respectively,

$N_{38}(t)$ and $N_{49}(t)$ = time dependent atom densities of ^{238}Np and ^{239}Pu respectively, atoms/cm³,

σ_{38}^f and σ_{49}^f = thermal fission cross section for ^{238}Np and ^{239}Pu respectively, barns,

ϕ_f = fast neutron flux (> 6.8 Mev) per unit fission neutron source density generated in Np assembly, $\frac{\text{cm}}{\text{sec}}$,

$\sigma_{37}^{n,2n}$ = n,2n cross section for ^{237}Np , barns.

4. External (n,2n) Reaction

The reaction rate from high energy neutrons generated externally to the target, R_4 , can be expressed as:

$$R_4 = \frac{dN_{36}^{(4)}}{dt} = N_{37}(t) \sigma_{37}^{n,2n} \phi_{ef}(t), \quad (4)$$

where:

$\phi_{ef}(t)$ = time dependent fast neutron flux generated external to the ^{237}Np assembly.

Total ^{236}Pu Concentration

All of the 22 hr ^{236}Np isomer does not beta decay to ^{236}Pu . About 50 percent decays by electron capture to ^{236}U . A long lived isomer (half life = 5×10^3 y) of ^{236}Np is formed and adds about 15% to the total ^{236}Np but not to ^{236}Pu formed during irradiation. Therefore, the rate of formation of the 22 hr isomer of ^{236}Np is expressed as:

$$\frac{dN_{36}}{dt} = (R_1 + R_2 + R_3 + R_4) - N_{36} \cdot (\lambda_{36} + \sigma_{36}^a \phi_{th}) \quad (5)$$

where:

- N_{36} = Time dependent ^{236}Np concentration,
 R_1 = Internal γ, n formation rate,
 R_2 = External γ, n formation rate,
 R_3 = Internal $n, 2n$ formation rate,
 R_4 = External $n, 2n$ formation rate,
 σ_{36}^a = Microscopic absorption cross section for ^{236}Np ,
 ϕ_{th} = Time averaged thermal neutron flux.

From equation 5 the time rate of change of ^{236}Pu is:

$$\frac{dN_{46}}{dt} = 0.5 \lambda_{36} \cdot N_{36} - N_{46} \sigma_{46}^a \cdot \phi_{th} \quad (6)$$

where:

- N_{46} = time dependent concentration of ^{236}Pu ,
 σ_{46}^a = absorption cross section of ^{236}Pu .

The decay of ^{236}Pu by α emission was not included in the analysis because of its long half-life -- 2.4 years compared to irradiation times of weeks. Using equations 1, 2, 3, 4, 5, and 6 the time dependent concentration of ^{236}Pu can be determined. Equations 5 and 6 were solved using standard Runge-Kutta methods. Each of the contributions to the $^{236}\text{Pu}/^{238}\text{Pu}$ ratio, corrected for burnup, can be expressed as follows:

$$\text{Internal } (\gamma, n) = K_1 \cdot \frac{N_{36}^{(1)}}{N_{48}}, \quad (7)$$

$$\text{External } (\gamma, n) = K_1 \cdot \frac{N_{36}^{(2)}}{N_{48}}, \quad (8)$$

$$\text{Internal (n,2n)} = K_1 \cdot \frac{N_{36}^{(3)}}{N_{48}}, \quad (9)$$

$$\text{External (n,2n)} = K_1 \cdot \frac{N_{36}^{(4)}}{N_{48}}$$

where: K_1 = the ratio of the total amount of ^{236}Pu with burnup included in the analysis to the total amount of ^{236}Pu with no burnup included,

N_{48} = concentration of ^{238}Pu after irradiation,

$N^{(1)}, N^{(2)}, N^{(3)}, N^{(4)}$ = concentrations of ^{236}Pu from the indicated reactions assuming no burnup.

This calculational procedure differs slightly from the method discussed by W. E. Graves in DPST-70-356 in two ways. Reactions from particles generated externally and internally to the target are treated separately. This modification allows isolation of individual contributions to the $^{236}\text{Pu}/^{238}\text{Pu}$ ratio. Also, the ^{238}Pu production and ^{236}Pu burnup are calculated as part of the analysis.

Input Parameters

Sources of High Energy Gammas

There are two major contributors to the high energy gamma ray flux present in the reactor. The first comes from neutron capture in the aluminum components used in the core and target assemblies. The second originates from neutrons captured in the stainless steel tank wall. The magnitude of these fluxes is extremely sensitive to the types of SS and Al being used. For example, $\phi_\gamma, >6.8 \text{ Mev}$, from neutron captures in 8001 Al is approximately 30% greater than that from pure Al. Table II compares the γ yield ($>6.8 \text{ Mev}$) per 100 thermal neutron captures for typical Al used at SRL.

TABLE II

High Energy (>6.8 Mev) Gamma Yields per 100 Thermal
Neutron Captures

Al, Additives and Impurities	γ 's/100 Captures		
	Al(8001)	Al(6063)	Al(1100)
Al	33	33	33
Ni	7.7	0	0.07
Fe	1.81	0.42	1.69
Cu	1.69	0.56	5.63
B	<u>0.17</u>	<u>0.34</u>	<u>0.20</u>
Total	44.37	34.32	40.59

Neutron captures in the stainless steel tank (type 304), (e.g., Fe, Ni and Cr) generate high energy γ 's (>6.8 Mev), and therefore the composition of the stainless steel will effect ϕ_γ . Another factor is the extra energy component above 8 Mev which comes, from each of the components of the stainless steel.^(3,4) This two-energy group analysis is not necessary for Al unless large amounts of type 8001 are used. It is clear from Table II that if the $^{236}\text{Pu}/^{238}\text{Pu}$ ratio is to be minimized 8001 Al should be used sparingly.

γ -Fluxes

Once the γ source strength in every region of the reactor is known, ϕ_γ in the ^{237}Np targets can be calculated. To accomplish this, either INCYCE or CLUCOP can be utilized.⁽⁵⁾ INCYCE and CLUCOP solve the integral transport equation

$$V_i \sum_1 \bar{\phi}_1 = \sum_{j=1}^N V_j (S_j + \sum_{S_j} \phi_j) P_{1j}, \quad (11)$$

where

V_i & V_j = Volumes of region i and j ,

Σ_i = Macroscopic one group total cross section for the i^{th} region,

Σ_{S_j} = Macroscopic one group scattering cross section for region j ,

S_j = Source density in region j ,

$\bar{\phi}_i, \bar{\phi}_j$ = Particle fluxes in regions i and j ,

$P_{i,j}$ = The probability that a particle originating with a uniform source distribution in region j will have its first collision in region i assuming zero current at the cell boundary,

N = Number of regions.

A discussion of how cross sections are selected as input for INCYCE and CLUCOP has been discussed previously,⁽¹⁾ however several points should be re-emphasized. The two dominant γ interactions, at energies above 1 Mev, with light and intermediate elements are Compton scattering and pair production. In pair production the gamma is lost and 2 particles are produced (an electron and a positron). Therefore, it can be considered an absorption. Compton scattering occurs when a γ interacts with an electron imparting a fraction of its energy to the electron. The γ is scattered with a reduced energy. In general, the reduced energy of the γ will be less than the 6.8 Mev threshold of the $^{237}\text{Np}(\gamma, n)$ reaction and therefore can also be considered as an absorption. The contribution from the externally generated γ flux, was calculated in two parts; the first from the contribution from gamma energies between 6.8 and 8.0 Mev, and the second for gammas above 8.0 Mev. This division was necessary because of the rapid increase in the $^{237}\text{Np} \sigma(\gamma, n)$ above the 6.8 Mev threshold and the contribution above 8 Mev from gammas generated by neutron captures in stainless steel.

The gamma fluxes for Cf-I given in Figure 1, were calculated with CLUCOP in the following manner. The reactor was divided into 10 concentric regions -- 3 core regions, 5 reflector regions, and 2 tank wall regions. Gamma ray source densities were calculated for each region. For the 3-region core:

$$\bar{\phi}_{th} = 2.23 \times 10^{15} \text{ n/cm}^2\text{-sec},$$

$$P_{max}/P_{ave} = 1.2.$$

The source density in any core region k can be expressed as:

$$S_1 = y \bar{\Sigma}_a(A1)\phi_1, \quad (12)$$

where

$$S_1 = \text{Source density, } \gamma'\text{'s/cm}^3\text{-sec},$$

$$y = \text{Gamma yield per capture for Al},$$

$$\bar{\Sigma}_a(A1) = \text{Core averaged Al absorption cross section, cm}^{-1},$$

$$\phi_1 = \text{Average thermal neutron flux for region 1, n/cm}^2\text{-sec}.$$

The Mark 18's make up approximately 80% of the assemblies in the core. Approximately 60% of the Al used in the Mark 18 is 6063; the remainder is 8001 Al. The other core assemblies are made of 6063-Al. Table III lists the cross sections, yields, and average source strengths in the core for both Al alloys.

TABLE III
Information For Gamma Ray Source Strengths Calculation
in the Cf-I Core

<u>Al</u>	<u>$\bar{\Sigma}_a(\text{cm}^{-1})$</u>	<u>$y(\gamma'\text{'s/capture})$</u>	<u>$Sv(\gamma'\text{'s/cm}^3\text{-sec}-\phi_{th})$</u>
8001	.000296	.444	.0001314
6063	.000567	.343	.0001948
Total			.0003262

The average cross sections used for Table III were derived from HAMMER cell calculations.

The source strength in the tank wall was calculated using 2 region - 1 group diffusion theory to determine the thermal flux distribution in the tank wall. As previously mentioned ϕ_γ from the wall was divided into 2 energy groups with an 8 Mev cutoff between groups. Table IV presents the yields for the two energy groups and the energy bounds for each group. (3)

TABLE IV
Gamma Source Strength Information in Tank Wall

	<u>Energy Bounds (Mev)</u>	<u>Yield (γ's/100 captures)</u>
Group 1	8.0 - 9.5	19.4
Group 2	6.8 - 8.0	44.2

A neutron absorption cross section of 0.22 cm^{-1} was used for the stainless steel. CLUCOP was also used to generate ϕ_γ from thermal neutron captures in the Np assemblies. One fundamental assumption in each of the CLUCOP calculations was that a zero albedo existed at the cell surface. This approximation should be very good because most of the γ 's scattered back would be at an energy less than the threshold of the $^{237}\text{Np}(\gamma, n)^{236}\text{Np}$ reaction. The average thermal fluxes used to calculate the internal γ source strength were determined using the $\phi_{\text{Np}}/\phi_{\text{core}}$ ratios (6) and reactor operations data. The γ fluxes generated externally, calculated by CLUCOP, are given in Table V.

TABLE V
Calculated External Gamma Fluxes

<u>Distance from core center, cm</u>	<u>Gamma Flux, $\gamma/\text{cm}^2\text{-sec}$ (6.8 - 8.0 Mev)</u>	<u>Gamma Flux, $\gamma/\text{cm}^2\text{-sec}$ (8.0 - 10.0 Mev)</u>
163*	6.13×10^{11}	1.33×10^{10}
210*	2.48×10^{11}	6.74×10^{10}
210	1.90×10^{11}	5.17×10^{10}
222	2.82×10^{11}	1.01×10^{11}
222	2.35×10^{11}	8.40×10^{10}
235	3.90×10^{11}	1.60×10^{11}

*Inner housings present

The rate of production of internal γ 's is proportional to the thermal flux and is dependent on the amounts and kinds of material present in an assembly. The γ fluxes internally generated for the 6 test assemblies are given in Table VI.

TABLE VI
Calculated Internal Gamma Fluxes

<u>Distance from core center, cm</u>	<u>Gamma Flux, $\gamma/\text{cm}^2\text{-sec}$ (6.8 Mev)</u>
163*	3.91×10^{12}
210*	1.42×10^{12}
210	7.01×10^{11}
222	5.49×10^{11}
222	4.57×10^{11}
235	2.38×10^{11}

*Inner housings present.

Production Cross Sections

Effective cross sections used for the production calculations were computed using the HAMMER library, and are listed in Table VII.⁽⁶⁾

TABLE VII
Np and Pu Cross Sections - 60°C

<u>Isotope</u>	<u>σ_a, barns</u>	<u>σ_f, barns</u>
^{237}Np	139	-
^{238}Np	1818	1658
^{239}Np	47	-
^{238}Pu	416	11.9
^{239}Pu	947	655

12/30/70

The absorption cross section for ^{236}Pu was taken to be 170 b at 60°C. (7) This cross section, as well as σ_a^{236} , $\sigma_{n,2n}^{236}$, and $\sigma_{\gamma,n}^{236}$ are not well known. The value of σ_a^{236} is felt to be accurate to +50%. The only other cross section on which there are any data is $\sigma_{n,2n}^{236}$. However, its energy dependence comes from a theoretical treatment, and could be considerably in error. This problem, plus the lack of information concerning the shape of the fission spectrum above 7 Mev for any fissile material, makes estimates of $\sigma_{n,2n}^{236}$ approximate at best. Fortunately, this reaction represents only a small part of the total ^{236}Np production (15% maximum). Therefore, errors in $\sigma_{n,2n}^{236}$ will not affect this analysis significantly. The fission-spectrum-averaged value of $\sigma_{n,2n}^{236}$ used was 56 mb. (1) The absorption cross section of ^{236}Np is also unknown. However, various values from 400 to 2500 barns were used in the analysis, and little effect on the total ^{236}Pu concentration was observed.

The $\sigma_{\gamma,n}^{236}$ cross section, therefore, was used as a fitting parameter which could be varied to provide a value of the $^{236}\text{Pu}/^{238}\text{Pu}$ ratio consistent with experimental data. Because of the γ -ray spectra from neutron capture in Al, Fe and Ni two energy groups were chosen 6.8 to 8.0 Mev and >8.0 Mev. Isolating a consistent value for the lower energy group was reasonably simple because the contribution to the ^{236}Np from the external gamma and internal gamma sources for the test irradiation position nearest the Cf-I core center, 163 cm, was due almost entirely to the lower energy γ 's. The (γ,n) cross section for the high energy group was determined using the irradiation point nearest the tank wall. The high energy gamma flux is largest at this point. The 2-group (γ,n) cross sections used for all the calculations presented in this memorandum are:

$$\sigma_{\gamma,n}^{(1)} = 15.2 \text{ mb} \quad 6.8 - 8.0 \text{ Mev,}$$

$$\sigma_{\gamma,n}^{(2)} = 68.1 \text{ mb} \quad 8.0 - 10.0 \text{ Mev.}$$

Results

^{237}Np Test Irradiations in Cf-I

Six test assemblies were irradiated in the reflector at 4 different radii. Two of the assemblies had inner aluminum housings for forced cooling. The positions of the assemblies and the experimental results are given in Table VIII. Also included are the calculated thermal neutron fluxes. (6)

TABLE VIII

Experimental $^{236}\text{Pu}/^{238}\text{Pu}$ Ratios and Average Thermal Fluxes

<u>Distance from core center, cm</u>	<u>$^{236}\text{Pu}/^{238}\text{Pu}$</u>	<u>$\bar{\phi}$, n/cm²-sec</u>	<u>Reactor Cycles</u>
163*	0.43	8.4×10^{14}	1
210*	0.39	3.0×10^{14}	1
210	0.35	2.3×10^{14}	5
222	0.41	1.8×10^{14}	2
222	0.47	1.5×10^{14}	5
235	0.98	0.8×10^{14}	5

*Inner housings present.

Using the calculated γ fluxes in Table V and VI along with average thermal neutron flux values given in Table VIII, the relative contributions to the $^{236}\text{Pu}/^{238}\text{Pu}$ ratio and their total are compared to the experimental values in Table IX.

TABLE IX

^{237}Np Test Irradiations in Cf-I
Contributions to $^{236}\text{Pu}/^{238}\text{Pu}$ Ratio, ppm
Calculated Compared to Experimental

<u>Distance from core center, cm</u>	<u>In(γ,n) >6.8 Mev</u>	<u>Ex(γ,n) >8.0 Mev</u>	<u>Ex(γ,n) <8.0 Mev</u>	<u>In(n,2n)</u>	<u>Ex(n,2n)</u>	<u>Calc Total</u>	<u>Exper Total</u>
163*	0.32	0.004	0.045	0.06	0	0.43	0.43
210*	0.29	0.06	0.04	0.02	0	0.41	0.39
210	0.21	0.06	0.05	0.03	0	0.35	0.35
222	0.196	0.14	0.085	0.02	0	0.044	0.41
222	0.20	0.15	0.09	0.02	0	0.46	0.47
235	0.19	0.51	0.27	0.01	0	0.98	0.98

An estimate of the validity of the calculational method can be made by comparing the statistic S_e^2 , the standard error of estimate, with S_e^2 obtained from least squares analysis of the 6 test irradiations.

$$S_e^2 = \frac{1}{n-2} \sum_{i=1}^n (y_i - z_i)^2 \quad (13)$$

where:

n = number of data points,

y_i = experimental value,

z_i = calculated value.

Comparing the calculated and experimental $^{236}\text{Pu}/^{238}\text{Pu}$ ratios gives $S_e^2 = 3.75$. A least squares analysis gives $S_e^2 = 7.5$. This indicates that the calculated $^{236}\text{Pu}/^{238}\text{Pu}$ ratios are in better agreement with the experimental values than the least squares values.

Foil Irradiations in Cf-I

$^{237}\text{NpO}_2$ was placed in Zr capsules which were housed in a Zr assembly and irradiated in Cf-I. (9) Six such assemblies were irradiated. Zr was used to remove most of the internally generated (γ, n) reactions. A reliable theoretical analysis of these irradiations is difficult because the γ sources distribution could not be duplicated exactly in the transport codes. Therefore, the calculated $\text{In}(\gamma, n)$ contribution could be approximately a factor of 2 too low. The calculated results are given in Table X along with experimental values determined using alpha counting.

TABLE X

Contributions to $^{236}\text{Pu}/^{238}\text{Pu}$ Ratio for Zr Test Irradiations, ppm

Distance from core center, cm	$\text{In}(\gamma, n)$ >(6.8 Mev)	$\text{Ex}(\gamma, n)$ >8.0 Mev	$\text{Ex}(\gamma, n)$ ≤8.0 Mev	$\text{In}(n, 2n)$	Calc. Total	Experimental Total
195	0.01	0.03	0.05	0.04	0.13	0.19
190	0.01	0.025	0.045	0.04	0.13	0.12

The experimental values have been corrected for the significant contribution from the residue $^{236}\text{Pu}/^{238}\text{Pu}$ ratio initially present in the neptunium.

Mark 61 Irradiations - Plant Production Program

Before the $^{236}\text{Pu}/^{238}\text{Pu}$ ratio for the plant product can be calculated, the effect of the 24 Mark 61 assemblies on the thermal neutron flux at the tank wall had to be determined. From previous calculations⁽⁶⁾ it was shown that the neutron flux in the assemblies was depressed by approximately 30%. However, using a series of HAMMER-HERESY calculations, it was found that the thermal neutron flux at the tank wall recovered to within 5% of the value with no Mark 61 assemblies present.

The Mark 61 assemblies differ from the original six test assemblies as shown in Table XI.

TABLE XIComparison of the Mark 61 and the Test Assembly

	<u>Mk 61</u>	<u>Test Assembly</u>
Loading, g/ft.	40	40
Clad thickness, mils	20	30
Core thickness, mils	30	45
Inner diameter, in.	4.01	4.01

The Mark 61 assemblies were irradiated at 198 and 202 cm from the core center. These positions were chosen to minimize external (γ, n) reactions and still remain below heat removal limits. Thermal neutron fluxes at each position again were determined as before. The Mark 61's were irradiated for 5 reactor cycles to achieve a ^{237}Np burnup of approximately 9.0%. The external gamma fluxes at each radial position, for a nominal average core thermal flux of 3.26×10^{15} n/cm²-sec are given in Table XII.

TABLE XII

Average External γ Fluxes at Mark 61's, $\gamma/\text{cm}^2\text{-sec}$

Position, cm	Gamma Flux (>8.0 Mev)	Gamma Flux (6.8 - 8.0 Mev)
198	4.88×10^{10}	2.94×10^{11}
202	4.69×10^{10}	2.90×10^{11}

The internal average γ fluxes 6.8 Mev are 9.86×10^{11} $\gamma/\text{cm}^2\text{-sec}$ at 198 cm and 9.00×10^{11} $\gamma/\text{cm}^2\text{-sec}$ at 202 cm. The contributions to the $^{236}\text{Pu}/^{238}\text{Pu}$ ratio are given in Table XIII.

TABLE XIII

Contributions to $^{236}\text{Pu}/^{238}\text{Pu}$ Ratio for Plant Product, ppm

Position	In(γ, n) >6.8 Mev	Ex(γ, n) <8.0 Mev	Ex(γ, n) >8.0 Mev	In($n, 2n$)	Total
198	0.16	0.045	.036	0.06	0.30
202	0.15	0.05	0.05	0.05	0.30

ObservationsTarget Design

The design of the target assembly is important to minimize the $^{236}\text{Pu}/^{238}\text{Pu}$ ratio because:

- o The internally generated ϕ_γ is approximately proportional to the thickness of aluminum in the assembly.
- o ϕ_γ is dependent on additives and impurities in the Al.
- o The internally generated fast neutron flux, from ^{239}Pu and ^{238}Np fissions, is proportional to the ^{237}Np density.

Therefore minimizing the amount of Al in the housings and cladding of a ^{237}Np assembly is very desirable. However, minimizing the Al in the core of the target increases the ^{237}Np density for a constant loading, the latter could increase the internally generated fast neutron flux, producing an increase in the ^{236}Pu concentration from (n,2n) reactions.

Materials

The $^{236}\text{Pu}/^{238}\text{Pu}$ ratio could be reduced to approximately 0.2 in reflector irradiations if the target core and 1/2 of the cladding of a Mark 61 assembly were Mg instead of Al. Mg is currently being studied as a replacement for Al. Zr could also be used as a substitute for Al again giving a $^{236}\text{Pu}/^{238}\text{Pu}$ ratio of 0.2.

When Al is used as structural material for ^{237}Np targets, alloys with high levels of additives and impurities should be avoided. Both 1100-Al and 8001-Al produce more high energy gammas per absorption than 6063-Al and therefore increase the ^{236}Pu production.

CKP:vpb

REFERENCES

- (1) W. E. Graves, Calculation of ^{236}Pu Contaminant In ^{238}Pu Product, DPST-70-356, 5/27/70.
- (2) Theoretical Physics Division Monthly Report, December 1969, DPST-69-114-12, Secret.
- (3) R. E. Maerker and F. J. Muckenthaler, Gamma Ray Spectra Arising From Thermal Neutron Capture in Elements Found in Soils, Concretes and Structural Materials, ORNL-4382.
- (4) Reactor Physics Constants, ANL-5800.
- (5) T. B. Martonen, Application of The CLUCOP Code, DPST-68-495.
- (6) T. C. Gorrell, Production of High Quality Grade ^{238}Pu in A Cf-I Blanket, DPST-70-251.
- (7) J. A. Smith, APE (Actinide Production Equations), Memorandum, 5/22/67.
- (8) C. E. Ahlfield and N. P. Baumann, A Direct Measurement of the (γ, n) Cross Section for ^{237}Np , ^{232}Th , and ^{233}U , DPST-69-551, 10/10/69.
- (9) F. B. Christensen, Medical ^{238}Pu Irradiations in Zirconium, DPSOX 7522, 3/11/70.

Figure 1

DPST-70-573

12/30/70

External Gamma Fluxes in CI-1 Reflector.

EUGENE DIETZGEN CO.
MADE IN U. S. A.

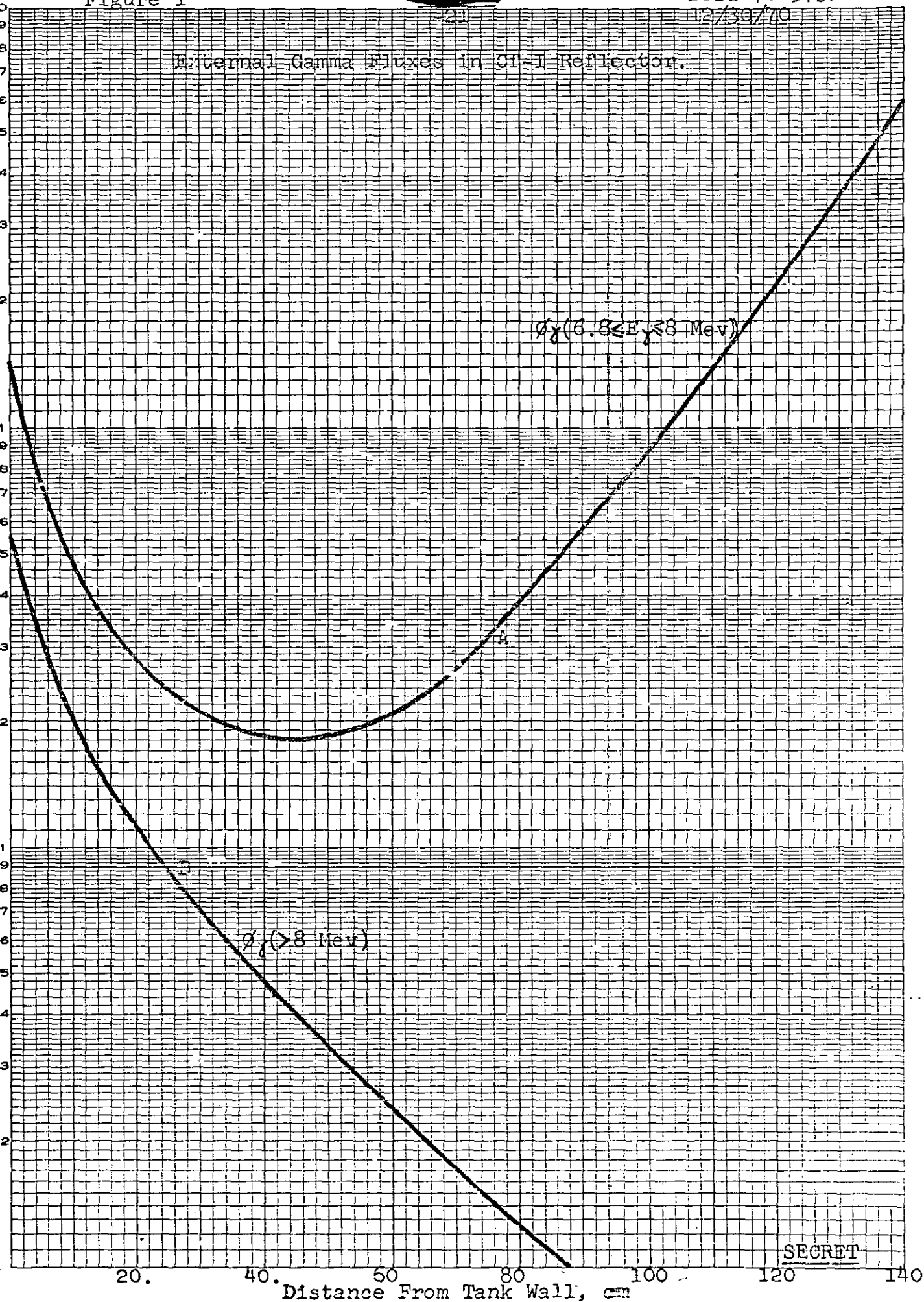
NO. 34DR-L31D DIETZGEN GRAPH PAPER
SEMI-LOGARITHMIC
3 CYCLES X 10 DIVISIONS PER INCH

$\phi \times 10^{-12}$

1.0

0.1

0.01



SECRET